ChemComm

COMMUNICATION

View Article Online
View Journal | View Issue

Cite this: *Chem. Commun.*, 2025, **61**, 19253

Received 9th September 2025,
Accepted 3rd November 2025

DOI: 10.1039/d5cc05209b

rsc.li/chemcomm

Modulating the thermal isomerization barriers of quadricyclane to norbornadiene through cross-conjugative patterns

Francisco Antonio Martins and Judy I-Chia Wu *

Computations show that thermal isomerizations of quadricyclane to norbornadiene can be modulated by heteroarene substitution. Heteroarenes that are non-cross-conjugated to the norbornadiene double bond increase delocalization of the transition state structure and lower the thermal activation enthalpy ($\Delta H^{\ddagger}$), while cross-conjugated analogs increase $\Delta H^{\ddagger}$ without significantly impacting the storage enthalpy ($\Delta H_{storage}$).

Molecular solar thermal energy storage (MOST) systems are photoswitchable molecules that store solar energy by converting light into chemical energy.[1] These systems typically exist as pairs of isomers that can reversibly convert through light-induced bond cleavage, bond rotation, or conformational changes. Common MOST frameworks include the *E*/*Z*-azobenzenes,[2,3] dihydroazulene–vinylheptafulvene,[4–6] dimetal fulvalene complexes,[7,8] and notably, the norbornadiene–quadricyclane (NBD–QC) pair.[9,10] A schematic illustration of the NBD–QC pair functioning as a MOST system is shown in Fig. 1a. Upon photoexcitation, NDB converts to the metastable QC. The energy difference of the two is the stored energy ($\Delta H_{storage}$), which can then be released spontaneously or by external stimuli (*e.g.*, heat, light,[2,3] or electric potential[11,12]) through a thermal back reaction barrier ($\Delta H^{\ddagger}$). Thermal relaxation of QC to NBD proceeds *via* a concerted, asynchronous, retro-[2+2] cycloaddition, and the transition state structure exhibits high diradical character.[13–15] Efficient MOST systems must meet several criteria: (I) absorption within the solar window; (II) a high photoisomerization quantum yield; (III) a high energy density; (IV) a high energy storage, and (V) a long thermal half-life for the metastable isomer (*i.e.*, a suitable thermal back reaction barrier, $\Delta H^{\ddagger}$).[9,16] These features can be modified through structural designs of the MOST framework, but often, improving some criteria comes at the expense of others.

Norbornadiene stands out among common MOST systems for its low molecular weight and high energy density (0.97 MJ kg^{-1}),[17] but its absorption maximum lies outside of the solar window.[18] Structural modifications of NBD–QC have been explored to improve performance, for example, by placing donor (D) and acceptor (A) pairs through-space,[16] (Fig. 1b) or through-bond[19] (Fig. 1c), placing bulky substituents at the C7 bridge, (Fig. 1d)[20] or by heteroatom substitution (Fig. 1e).[21] One way to red-shift the absorption maxima is by tethering conjugated units to NBD, but this increases the molecular weight and reduces the energy storage per unit mass.[20] It was found that bulky groups at the C7 bridge could introduce steric stress, improving the quantum yield and increasing the thermal life-time of QC, although storage energy decreases modestly.[20] Enhanced storage enthalpies, $\Delta H_{storage}$,[22] and red-shifted absorptions[17] often correlate with reduced thermal isomerization barriers, $\Delta H^{\ddagger}$. Computational screening identified candidates with improved red-shift absorptions, storage capacity, and thermal half-lives.[23,24] Yet, strategies to maximize storage

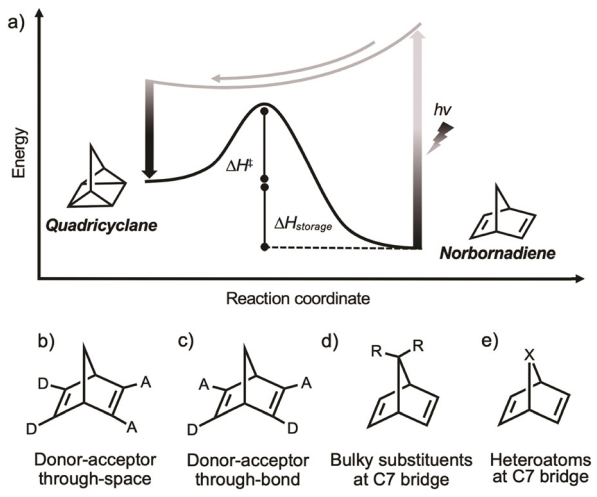

Fig. 1 (a) Schematic illustration of the photoisomerization of norbornadiene (NBD) and quadricyclane (QC). NBD motifs with donor (D) and acceptor (A) groups (b) through-space or (c) through-bond, and with modified C7 bridges by (d) alkyl (R) groups or (e) heteroatom (X = O or NH) substitution.

Department of Chemistry, University of Houston, Houston, Texas 77204-5003, USA. E-mail: jiwu@central.uh.edu

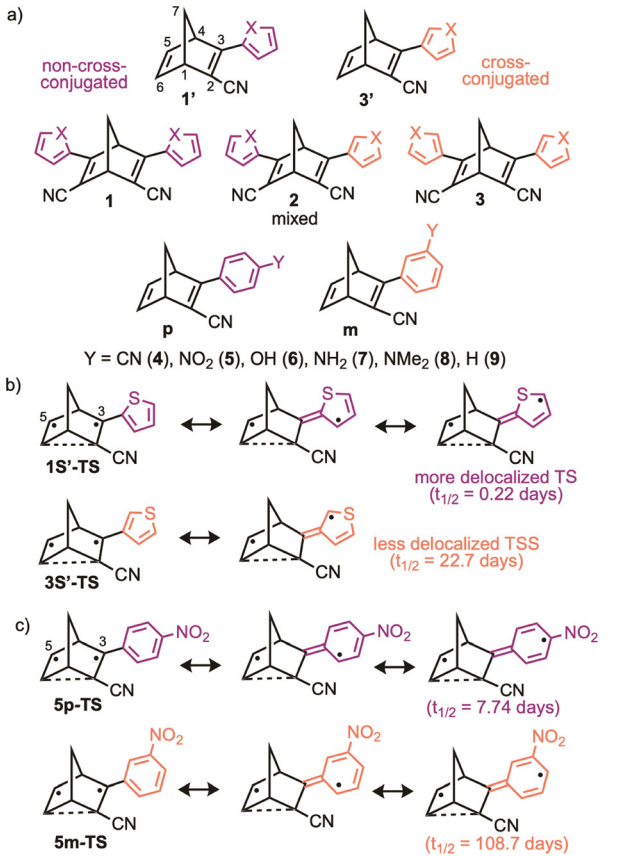

Fig. 2 (a) NBD frameworks investigated. (b) Resonance forms of **1S′-TS** *vs.* **3S′-TS** illustrate how non-cross-conjugative *vs.* cross-conjugative patterns affect delocalization of the unpaired electrons at the TS structure. (c) Resonance forms of **5p-TS** *vs.* **5m-TS** illustrate stabilization of unpaired electrons at the *para*-position. Thermal half-lives at 25 °C were taken from ref. 25.

enthalpies while targeting suitable storage half-lives remain elusive.

Here, we investigate the storage enthalpies ($\Delta H_{storage}$), thermal back reaction barriers ($\Delta H^{\ddagger}$), and computed absorption maxima (λ_{max}) for a series of NBD–QC frameworks containing through-bond donor–acceptor substituents (Fig. 2). Structures **1′** and **3′** were inspired by NBD–QC systems reported by Moth-Poulsen and co-workers, in which a π-accepting CN group is placed at C2 and a (hetero)arene is attached to C3; increasing donor strength and extending conjugation across the double bonds of NBD was found to increase storage half-lives from hours to days at room temperature.[22,25] Although the original work focused on the effects of *para*-substitution on $\Delta H^{\ddagger}$, the authors reported rather different thermal half-lives for **1S′** ($t_{1/2}$ = 0.22 days) *vs.* **3S′** (22.7 days) and for **5p** (7.74 days) *vs.* **5m** (108.7 days), at room temperature, which caught our attention.

We wondered whether the contrasting thermal stability of **1S′-QC** *vs.* **3S′-QC** might be explained by differences in their conjugation patterns. We noted that, in **1S′**, the two double bonds in the thiophene ring are non-cross-conjugated with the NBD double bond. Therefore, the transition state (TS) structure for the QC → NBD isomerization can be stabilized by delocalization of the unpaired electrons to the heteroarene, resulting in a lower $\Delta H^{\ddagger}$ and shorter thermal half-life (Fig. 2b, top, in purple). In **3S′**, the two double bonds of the thiophene ring are cross-conjugated with the NBD double bond. Thus, the QC → NBD TS structure is less stabilized by delocalization of the unpaired electrons, giving rise to a higher $\Delta H^{\ddagger}$ and longer thermal half-life (Fig. 2b, bottom, in orange). A similar explanation was put forth by Adrion and Lopez to rationalize the thermal half-lives of azoarenes.[26]

We expect that non-cross-conjugative *vs.* cross-conjugative patterns may provide a means to modulate $\Delta H^{\ddagger}$ barriers and tested our hypothesis by investigating a series of heteroarenes tethered to the double bond(s) of CN-substituted NBD frameworks, **1′** and **3′**; CN group placed at the C2 position, and an heteroarene (X = NH, O, S) attached to the C3 position. We also investigated NBD frameworks containing two sets of through-bond donor–acceptor pairs; two CN groups placed at the C2 and C6 positions of NBD, and two heteroarenes (X = NH, O, S) placed at C3 and C5. In structure **1**, the heteroarene double bonds are non-cross-conjugated to the NBD double bonds. In structure **2**, a mixed set of non-cross-conjugated and cross-conjugated heteroarenes are tethered to the NBD double bonds. In structure **3**, the heteroarene double bonds are cross-conjugated to the NBD double bonds.

Following the suggestion of one reviewer, we further examined a series of *para*- and *meta*-phenyl substituted 2-cyano-3-phenyl-NBD derivatives (**4**–**8**). Replacing the five-membered heterocycles by a phenyl group increases the thermodynamic penalty for dearomatization, resulting in modestly higher activation enthalpies for the thermal back reaction (Table 1). As shown in Fig. 2c, the TS structure for the QC → NBD isomerization can be further stabilized by π-donating or π-accepting substituents at the *para*-position, but not at the *meta*-position. As a result, 2-cyano-3-phenyl-NBD frameworks with *para*-substituted phenyl groups exhibit lower $\Delta H^{\ddagger}$ and shorter thermal half-lives compared to their *meta*-substituted counterparts (see Y = NO_2 example in Fig. 2c).

Computations for $\Delta H^{\ddagger}$ and $\Delta H_{storage}$ values were carried out at the CAM-B3LYP-D3(BJ)/6-311+G(d,p)//(U)PBE0-D3(BJ)/def2-TZVPP level, following the protocols of previous benchmarking studies.[20] Jorner *et al.* reported that computed $\Delta H^{\ddagger}$ and $\Delta H_{storage}$ values for the parent NBD–QC pair, based on single-point CAM-B3LYP energies and PBE0 geometries, agreed satisfactorily with CASPT2 energies and with experimental data.[15,20] The computed $\Delta H^{\ddagger}$ values for **1S′**, **3S′**, **5p**, **5m**, **8p**, and **9** correlate satisfactorily with experimental values measured in toluene at 25 °C (R^2 = 0.754), displaying a standard error of ± 0.63 (see Table 1 footnote and correlation plot in Fig. S4). However, direct comparisons of the computed and experimental $\Delta H^{\ddagger}$ indicate that the computed values are systematically underestimated, as found previously.[25] Absolute values for spin densities at the C3 and C5 positions were computed for the QC → NBD TS using the Natural Bond Orbital (NBO) program[27] at (U)PBE0-D3(BJ)/def2-TZVPP. Averaged absolute spin density values at the C3 and C5 positions, $|\delta_{avg}| = (|\delta_{C3}| + |\delta_{C5}|)/2$, indicate the extent of delocalization of the unpaired electrons. Absorption maxima (λ_{max}) for all substituted NBD and QC derivatives were computed at TD-PBE0-D3(BJ)/def2-TZVPP.

Table 1 Computed activation enthalpies ($\Delta H^{\ddagger}$), storage enthalpies ($\Delta H_{storage}$), averaged absolute spin density values at the C3/C5 positions ($|\delta_{avg}|$) of the TS structure, absorption maxima (λ_{max}, nm), and absorption intensity at λ_{max} (f). All energies are in kcal mol^{-1}

	$\lvert\delta_{avg}\rvert$	$\Delta H^{\ddagger}$	$\Delta H_{storage}$	QC λ_{max}	NBD λ_{max}	NBD f_{max}
Parent	0.84	31.1	−20.9	185.7	246.5	0.000
1NH′	0.67	19.4	−28.7	248.8	333.5	0.272
1O′	0.65	19.2	−25.7	241.3	334.4	0.254
1S′	0.65	20.1[a]	−25.0	253.1	337.5	0.245
3NH′	0.71	22.6	−26.8	236.2	321.3	0.144
3O′	0.70	22.8	−24.9	226.6	317.9	0.103
3S'	0.70	22.5[a]	−24.6	238.4	325.2	0.151
1NH	0.52	9.7	−34.6	307.1	409.1	0.040
1O	0.49	7.1	−33.3	287.6	394.4	0.041
1S	0.50	8.2	−31.7	294.9	402.4	0.035
2NH	0.56	11.0	−35.8	292.9	386.3	0.042
2O	0.54	10.9	−32.3	283.5	381.8	0.040
2S	0.54	12.7	−30.9	272.6	385.6	0.031
3NH	0.60	14.0	−34.1	284.3	372.1	0.023
3O	0.59	14.7	−31.2	264.4	359.5	0.012
3S	0.58	14.9	−30.2	369.6	369.6	0.025
4p	0.68	22.4	−23.1	335.5	335.5	0.214
4m	0.70	23.3	−23.2	324.7	324.7	0.120
5p	0.67	22.3[a]	−22.8	352.3	352.3	0.218
5m	0.70	23.2[a]	−23.2	346.3	346.3	0.030
6p	0.70	23.0	−25.0	325.2	325.2	0.273
6m	0.70	23.4	−23.6	323.9	323.9	0.146
7p	0.69	22.3	−25.5	337.8	337.8	0.378
7m	0.70	23.2	−24.1	353.0	353.0	0.067
8p	0.68	22.2[a]	−25.8	354.0	354.0	0.499
8m	0.70	23.5	−24.2	395.1	395.1	0.036
9	0.70	23.2[a]	−23.9	241.7	317.3	0.171

[a] Experimental $\Delta H^{\ddagger}$ values (in kcal mol^{-1}) for **1S′** (22.8), **3S′** (25.8), **5p** (24.1), **5m** (28.0), **8p** (26.4), **9** (26.8) were derived from the Eyring equation, based on measurements at 25 °C in toluene.[22,25]

Direct comparisons of pairs of cross-conjugated *vs.* non-cross-conjugated species show that π-conjugation patterns can largely affect electron delocalization of the QC → NBD TS structure (Table 1). Consistent with the schematic illustration shown in Fig. 2b, $|\delta_{avg}|$ values for the non-cross-conjugated TS structures, **1NH′** (0.67), **1O′** (0.65), **1S′** (0.65), are smaller than those of the cross-conjugated isomers, **3NH′** (0.71), **3O′** (0.70), **3S′** (0.70), indicating increased delocalization in **1NH′**, **1O′**, **1S′**. At the TS structure, non-cross-conjugated species exhibit more delocalization (*i.e.*, less spin at C3 and C5, *cf.* Fig. 2b, top, in purple), while cross-conjugated species display less delocalization (*i.e.*, more spin at C3 and C5, *cf.* Fig. 2b, bottom, in orange). Accordingly, computed $\Delta H^{\ddagger}$ barriers for the non-cross-conjugated, **1NH′** (19.4 kcal mol^{-1}), **1O′** (19. 2), **1S′** (20.1), are lower compared to those of their cross-conjugated isomers, **3NH′** (22.6), **3O′** (22.8), **3S′** (22.5). Increased thermal stability of QC (*i.e.*, a larger $\Delta H^{\ddagger}$) correlates with a decreased storage enthalpy (*i.e.*, a less negative $\Delta H_{storage}$).[20,28,29] Thus, the computed $\Delta H_{storage}$ values for **1NH′** (−28.7 kcal mol^{-1}), **1O′** (−25.7), and **1S′** (−25.0), are more exothermic than that of **3NH′** (−26.8), **3O′** (−24.9), and **3S′** (−24.6). Nevertheless, we note that a meaningful increase in $\Delta\Delta H^{\ddagger}$ (3.2, 3.6, 2.4 kcal mol^{-1}, respectively, for **1NH′** *vs.* **3NH′**, **1O′** *vs.* **3O′**, and **1S′** *vs.* **3S′**) only is accompanied by a comparably small change in $\Delta\Delta H_{storage}$ (1.9, 0.8, 0.4 mol^{-1}, respectively, for **1NH′** *vs.* **3NH′**, **1O′** *vs.* **3O′**, and **1S′** *vs.* **3S′**). These results suggest that it is possible to modulate $\Delta H^{\ddagger}$ without significantly compromising $\Delta H_{storage}$.[20]

NBD frameworks containing two sets of through-bond donor–acceptor pairs (**1**, **2**, and **3**, X = NH, O, S) display even more pronounced spin delocalization and barrier lowering effects. Isomers with two non-cross-conjugated heteroarenes tethered to the double bonds of NBD, **1** (X = NH, O, S), have largely delocalized unpaired electrons at the TS structure. This is followed by isomers with a mixed conjugative pattern, **2** (X = NH, O, S). Isomers with two cross-conjugated heteroarenes tethered to the double bonds of NBD, **3** (X = NH, O, S), display the least delocalized unpaired electrons at the TS structure. Indeed, computed $|\delta_{avg}|$ values for the non-cross-conjugated: **1NH** (0.52), **1O** (0.49), **1S** (0.50), are smaller than those computed for isomers of the mixed set: **2NH** (0.56), **2O** (0.54), **2S** (0.54), while values for the cross-conjugated isomers: **3NH** (0.60), **3O** (0.59), **3S** (0.58) are the highest, indicating decreased delocalization of the unpaired electrons (Table 1). Notably, computed $\Delta H^{\ddagger}$ barriers for **1NH** (9.7 kcal mol^{-1}), **1O** (7.1), **1S** (8.2) are lower than that computed for the mixed set: **2NH** (11.0), **2O** (10.9), **2S** (12.7), while the cross-conjugated isomers, **3NH** (14.0), **3O** (14.7), **3S** (14.9), display the highest $\Delta H^{\ddagger}$ barriers. By comparing examples from the two extreme cases, **1** *vs.* **3**, we note again that a meaningful increase in $\Delta\Delta H^{\ddagger}$ (4.3, 7.6, and 6.7 kcal mol^{-1}, respectively, for **1NH** *vs.* **3NH**, **1O** *vs.* **3O**, and **1S** *vs.* **3S**) only is accompanied by a small decrease in $\Delta\Delta H_{storage}$ (0.5, 2.1, 1.5 kcal mol^{-1}, respectively, for **1NH** *vs.* **3NH**, **1O** *vs.* **3O**, and **1S** *vs.* **3S**).

Computed activation enthalpies ($\Delta H^{\ddagger}$), storage enthalpies ($\Delta H_{storage}$), and $|\delta_{avg}|$ values for the 2-cyano-3-phenyl-NBD derivatives support that stabilizing the unpaired electrons at the *para*-positions of the phenyl group lower $\Delta H^{\ddagger}$. *Para*-substituted analogs enable more efficient delocalization from the NBD core to the phenyl ring, and therefore display consistently lower $|\delta_{avg}|$ values than the parent **9** (0.70) and the *meta*-substituted analogs: **4p** (0.68) < **4m** (0.70), **5p** (0.67) < **5m** (0.70), **6p** (0.70) ≈ **6m** (0.70), **7p** (0.69) < **7m** (0.70), and **8p** (0.68) < **8m** (0.70). Accordingly, the computed $\Delta H^{\ddagger}$ barriers are lower for the *para*-isomers than for **9** (23.2 kcal mol^{-1}) and the *meta*-isomers: **4p** (22.4) < **4m** (23.3), **5p** (22.3) < **5m** (23.2), **6p** (23.0) < **6m** (23.4), **7p** (22.3) < **7m** (23.2), and **8p** (22.2) < **8m** (23.5).

Finally, an effective MOST system also must absorb within the solar spectrum (*i.e.*, between 300 to 700 nm). However, strategies that red-shift the absorption of NBD often also red-shift that of QC, which compromises the efficiency of photoconversion. As shown in Table 1, all of the NBD derivatives have absorption maxima at regions above 300 nm, while those the QC derivatives absorb at regions near or below 300 nm. We note that the non-cross-conjugated species are modestly red-shifted compared to their cross-conjugated analogs, but the variations are small (less than 20 nm). This suggests that the choice of incorporating non-cross-conjugated *vs.* cross-conjugated motifs has a minor effect on the absorption wavelength of NBD–QC systems. Interestingly, computed UV spectra indicate that NBD species with non-cross-conjugated motifs generally exhibit stronger absorption intensities (f_{max}) than those with cross-conjugated motifs. Similarly, within the 2-cyano-3-phenyl-NBD framework, *para*-substituted phenyl groups with π-donating or π-accepting substituents have higher absorption intensities compared to the *meta*-substituted

derivatives. Plots of λ_{max} *vs.* $\Delta H^{\ddagger}$ (R^2 = 0.691) show some correlation between the maximum absorption wavelengths of the NDB structure and the activation enthalpies. Additional correlation plots are included to the SI Fig. S5.

An excellent correlation was found between computed $|\delta_{avg}|$ values for the QC → NBD TS structures *vs.* the thermal back reaction barriers ($\Delta H^{\ddagger}$) for all investigated compounds (R^2 = 0.977, see data in SI). Yet, what do these calculations tell us about how to design effective MOST NBD–QC systems? The substituted NBD–QC systems investigated here meet several MOST criteria: they absorb within the solar window, exhibit high energy densities, and have meaningfully storage energies. A few structural features were identified as likely to prolong the thermal half-life of the QC → NBD transformation, including heteroarenes with cross-conjugative relationships to the NBD double bond and *meta* substituted phenyl groups. These insights offer practical chemical handles for the design of NBD–QC-based MOST systems and may be extend to other MOST frameworks with thermal back reactions that proceed through transition states with pronounced diradicaloid character.

The authors thank the National Institute of General Medical Sciences (NIGMS) of the National Institutes of Health (R35GM133548) for funding support. We also acknowledge use of the Carya and Sabine clusters as well as support from the Research Computing Data Core at the University of Houston.

Conflicts of interest

There are no conflicts to declare.

Data availability

The data supporting this article have been included as part of the supplementary information (SI). Supplementary information is available.See DOI: **https://doi.org/10.1039/d5cc05209b**.

Notes and references

1 A. Lennartson, A. Roffey and K. Moth-Poulsen, *Tetrahedron Lett.*, 2015, **56**, 1457.
2 L. Dong, Y. Feng, L. Wang and W. Feng, *Chem. Soc. Rev.*, 2018, **47**, 7339.
3 Z. Wang, R. Losantos, D. Sampedro, M. Morikawa, K. Börjesson, N. Kimizuka and K. Moth-Poulsen, *J. Mater. Chem. A*, 2019, **7**, 15042.
4 J. Mogensen, O. Christensen, M. D. Kilde, M. Abildgaard, L. Metz, A. Kadziola, M. Jevric, K. V. Mikkelsen and M. B. Nielsen, *Eur. J. Org. Chem.*, 2019, 1986.
5 M. Cacciarini, A. B. Skov, M. Jevric, A. S. Hansen, J. Elm, H. G. Kjaergaard, K. V. Mikkelsen and M. B. Nielsen, *Chem. – Eur. J.*, 2015, **21**, 7454.
6 A. B. Skov, S. L. Broman, A. S. Gertsen, J. Elm, M. Jevric, M. Cacciarini, A. Kadziola, K. V. Mikkelsen and M. B. Nielsen, *Chem. – Eur. J.*, 2016, **22**, 14567.
7 Y. Kanai, V. Srinivasan, S. K. Meier, K. P. C. Vollhardt and J. C. Grossman, *Angew. Chem., Int. Ed.*, 2010, **49**, 8926.
8 K. Börjesson, D. Ćoso, V. Gray, J. C. Grossman, J. Guan, C. B. Harris, N. Hertkorn, Z. Hou, Y. Kanai, D. Lee, J. P. Lomont, A. Majumdar, S. K. Meier, K. Moth-Poulsen, R. L. Myrabo, S. C. Nguyen, R. A. Segalman, V. Srinivasan, W. B. Tolman, N. Vinokurov, K. P. C. Vollhardt and T. W. Weidman, *Chem. – Eur. J.*, 2014, **20**, 15587.
9 V. A. Bren, A. D. Dubonosov, V. I. Minkin and V. A. Chernoivanov, *Russ. Chem. Rev.*, 1991, **60**, 451.
10 A. D. Dubonosov, V. A. Bren and V. A. Chernoivanov, *Russ. Chem. Rev.*, 2002, **71**, 917.
11 E. Franz, A. Kunz, N. Oberhof, A. H. Heindl, M. Bertram, L. Fusek, N. Taccardi, P. Wasserscheid, A. Dreuw, H. A. Wegner, O. Brummel and J. Libuda, *ChemSusChem*, 2022, **15**, e202200958.
12 A. Goulet-Hanssens, M. Utecht, D. Mutruc, E. Titov, J. Schwarz, L. Grubert, D. Bléger, P. Saalfrank and S. Hecht, *J. Am. Chem. Soc.*, 2017, **139**, 335.
13 C. Qin, Z. Zhao and S. R. Davis, *J. Mol. Struct.: THEOCHEM*, 2005, **728**, 67.
14 M. J. Kuisma, A. M. Lundin, K. Moth-Poulsen, P. Hyldgaard and P. Erhart, *J. Phys. Chem. C*, 2016, **120**, 3635.
15 H. M. Frey, *J. Am. Chem. Soc.*, 1964, 365.
16 Z. Yoshida, *J. Photochem.*, 1985, **29**, 27.
17 X. An and Y. Xie, *Thermochim. Acta*, 1993, **220**, 17.
18 V. Gray, A. Lennartson, P. Ratanalert, K. Börjesson and K. Moth-Poulsen, *Chem. Commun.*, 2014, **50**, 5330.
19 J. Orrego-Hernández, A. Dreos and K. Moth-Poulsen, *Acc. Chem. Res.*, 2020, **53**, 1478.
20 K. Jorner, A. Dreos, R. Emanuelsson, O. El Bakouri, I. F. Galván, K. Börjesson, F. Feixas, R. Lindh, B. Zietz, K. Moth-Poulsen and H. Ottosson, *J. Mater. Chem. A*, 2017, **5**, 12369.
21 H. Altenbach, H. Martin, B. Mayer, M. Müller, D. Constant and E. Vogel, *Chem. Ber.*, 1991, **124**, 791.
22 M. Quant, A. Lennartson, A. Dreos, M. Kuisma, P. Erhart, K. Börjesson and K. Moth-Poulsen, *Chem. – Eur. J.*, 2016, **22**, 13265.
23 J. L. Elholm, A. E. Hillers-Bendtsen, H. Hölzel, K. Moth-Poulsen and K. V. Mikkelsen, *Phys. Chem. Chem. Phys.*, 2022, **24**, 28956.
24 N. Ree, M. Koerstz, K. V. Mikkelsen and J. H. Jensen, *J. Chem. Phys.*, 2021, **155**, 184105.
25 M. Jevric, A. U. Petersen, M. Mansø, S. K. Singh, Z. Wang, A. Dreos, C. Sumby, M. B. Nielsen, K. Börjesson, P. Erhart and K. Moth-Poulsen, *Chem. – Eur. J.*, 2018, **24**, 12767.
26 D. M. Adrion and S. A. Lopez, *Org. Biomol. Chem.*, 2022, **20**, 5989.
27 E. D. Glendening, J. K. Badenhoop, A. E. Reed, J. E. Carpenter, J. A. Bohmann, C. M. Morales, P. Karafiloglou, C. R. Landis and F. Weinhold, *NBO 7.0*, Theoretical Chemistry Institute, University of Wisconsin, Madison, 2018.
28 A. Dreos, K. Börjesson, Z. Wang, A. Roffey, Z. Norwood, D. Kushnird and K. Moth-Poulsen, *Energy Environ. Sci.*, 2017, **10**, 728.
29 A. Dreos, Z. Wang, J. Udmark, A. Ström, P. Erhart, K. Börjesson, M. B. Nielsen and K. Moth-Poulsen, *Adv. Energy Mater.*, 2018, **8**, 1703401.

